Document downloaded from:

http://hdl.handle.net/10251/159983

This paper must be cited as:

Collazo-Bigliardi, S.; Ortega-Toro, R.; Chiralt, A. (2019). Using grafted poly(epsilon-caprolactone) for the compatibilization of thermoplastic starch-polylactic acid blends. Reactive and Functional Polymers. 142:25-35. https://doi.org/10.1016/j.reactfunctpolym.2019.05.013

The final publication is available at

https://doi.org/10.1016/j.reactfunctpolym.2019.05.013

Copyright Elsevier

Additional Information

Using grafted poly(ε-caprolactone) for the compatibilization of thermoplastic starch-polylactic acid blends

Sofía Collazo-Bigliardi[a*], Rodrigo Ortega-Toro[b], Amparo Chiralt[a]

[a]Instituto de Ingeniería de Alimentos para el Desarrollo, Universidad Politécnica de Valencia, Camino de Vera s/n, 46022 Valencia, Spain. socol@alumni.upv.es; dchiralt@tal.upv.es

[b]Programa de Ingeniería de Alimentos, Facultad de Ingeniería, Universidad de Cartagena, Carrera 6 # 36-100, Cartagena de Indias D.T y C, Colombia. rortegap1@unicartagena.edu.co

*Corresponding author: Sofía Collazo-Bigliardi. Instituto de Ingeniería de Alimentos para el Desarrollo, Universidad Politécnica de Valencia, Camino de Vera s/n, 46022 Valencia, Spain. Phone: 34-963877924. Fax: 34-963877926. socol@alumni.upv.es

ABSTRACT

Thermoplastic starch (S) and polylactic acid (PLA) blend films were obtained by melt blending and compression moulding using grafted polycaprolactone with maleic anhydride and/or glycidyl methacrylate (PCL_{MG} or PCL_G) as compatibilizers. The effect of both the PLA ratio in the blend (20 and 40% with respect to starch) and the amount of both compatibilizers (2.5 and 5%) on the film properties was analysed. Compatibilized blends presented a better dispersion of the PLA in the continuous starch phase, but the use of PCL_G provoked a phase inversion in the matrix when 40% of the starch was substituted by PLA. The compatibilized blend films exhibited higher values

of elastic modulus than pure starch films, but were less extensible. The use of compatibilizers did not affect the film's water vapor permeability, which was reduced by up to 33 or 50% for 20 and 40% PLA, respectively, although inverted films with 40% PLA and 5% PCL_G, exhibited marked reduction (67%). Compatibilizers decreased the oxygen permeability of the films by about 50%, regardless of the ratio of PLA and the kind and amount of compatibilizer. Therefore, substituting 20% of the starch by PLA and incorporating 5% of PCL_G would be a good strategy to obtain films useful for food packaging.

Keywords: Starch, Polylactic acid, Grafted polycaprolactone, Compatibilizers, Blend films.

1. Introduction

Food packaging involves a high consumption of conventional plastics which generate large amounts of waste. These kinds of materials are the most widely used in the food industry due to their great versatility and optimum characteristics for food packaging. Nowadays, an important challenge is to develop different materials that contribute to minimising the environmental impact of petroleum-based plastics, making use of renewable sources, such as biopolymers [1, 2]. One of the most important groups of biodegradable polymers obtained from renewable resources is polysaccharides. These biopolymers are extracted directly from biomass and, depending on their origin, different types of starch, cellulose, chitosan, gums or alginates can be found [3,4]. Another predominant group of bioplastics is those obtained by synthesis from biobased monomers, such as polylactic acid (PLA), or non-biobased monomers, such as poly (ε-caprolactone) (PCL), polyvinyl alcohol (PVA) or polybutylenosuccinate (PBS) [5, 6].

Starch is one of the most widely studied biodegradable polymer for food packaging applications since it is suitable for food contact, abundant and low cost. Likewise, starch can be thermoprocessed by adding plasticizers, which provokes starch gelatinization and give rise to thermoplastic starch (TPS). TPS exhibits an excellent filmogenic capacity, forming homogeneous and transparent films, with high barrier capacity for oxygen, carbon dioxide or lipids [7]. However, it has certain drawbacks that limit its potential application, such as its high degree of water sensitivity and water vapour permeability, its limited mechanical properties and instability due to retrogradation during storage [8]. Different strategies have been used for the purposes of improving these properties: adding reinforcing agents [9, 10], incorporating cross-linking agents, such as citric acid, adding plasticizers to reduce intermolecular forces and increase flexibility or blending with other polymers [11]. As concerns the blends, the mixtures with more hydrophobic polymers, such as polylactic acid (PLA), have been widely studied in order to minimize the drawbacks of starch, although the lack of polymer compatibility makes the use of compatibilizers necessary [12].

Polylactic acid is linear aliphatic thermoplastic polyester derived from lactic acid, which is obtained from the fermentation of renewable and biodegradable sources (corn or rice starch and raw materials with high sugar content). It can be produced by the chemical conversion of these carbohydrate sources into dextrose; the dextrose is fermented to lactic acid followed by the polycondensation of lactic acid monomers [3]. PLA is biodegradable, renewable and biocompatible; it is also transparent and has excellent water vapor barrier properties [13]; these characteristics are comparable to those of petroleum-based plastics, such as polyethylene terephthalate (PET) or polystyrene (PS). Due to the new technologies available in the area of industrial production, the PLA has a very competitive price on the market. However, it has certain limitations, such as the

fact that it has a low oxygen barrier capacity and is brittle, despite being highly resistant to traction [14].

Both PLA and starch materials have opposite barrier and mechanical properties and the possibility of combining them to obtain matrices with improved properties can counteract the disadvantages shown by pure polymers. However, their insufficient compatibility gives rise to blends with phase separation that limits their effectiveness as packaging materials [15]. To improve the interfacial adhesion between the starch and hydrophobic polymer phases, compatibilizers, with an adequate fraction of polar and non-polar groups, have been added to promote polymer interfacial interaction, thus improving the properties of the blends. For this purpose, S-PLA blends have been compatibilized with citric acid (wheat flour-PLA), methylene diphenyl diisocytane (wheat starch-PLA), stearic acid (corn starch-PLA), maleic anhydride (potato starch-PLA), dicumyl peorxyde and maleic anhydride (corn starch-PLA), adipate or citrate esters (cassava starch-PLA), formamide (corn starch-PLA), maleic anhydride and epoxidized soybean oil (corn starch-PLA), among others [12]. Le Bolay et al. [16], combine PLA and starch in composite materials avoiding the use of compatibilizers or plasticizers through co-grinding, reducing the hydrophilic nature of the blend and the starch's polar energy component.

In previous studies [17, 18], biodegradable polyesters, such as poly-ε-caprolactone (PCL) were functionalized with polar groups, such as epoxide or anhydride, capable of positively interacting with the hydroxyl groups of the starch chains, exerting a positive effect on the polymer's compatibility. These compounds, therefore, act as coupling agents between both materials, improving their compatibility, due to their amphiphilic nature [19].

The aim of this study was to analyse the effectiveness of PCL, functionalized by grafting with maleic anhydride and/or glycidyl methacrylate, at improving the properties of blend films based on corn starch and PLA, obtained by melt blending and compression moulding. Films were characterized as to their microstructure, thermal behaviour and functional properties (mechanical, optical and barrier). The effect of the PLA ratio in the blend, as well as the amount of both compatibilizers, was analysed in order to select the best formulation for food packaging applications.

2. Materials and methods

2.1. Materials

Corn starch (28 % amylose) was provided by Roquette (Roquette Laisa, Benifaió, Spain), glycerol was obtained from Panreac Química, S.A. (Castellar del Vallès, Barcelona, Spain) and amorphous PLA 4060D, density of 1.24 g/cm3, was purchased from Natureworks (U.S.A). For the chemical modification of PCL (pellets ~3 mm, average Mn 80.000 Da, glycidyl methacrylate (G) (purity 97%), maleic anhydride (M) (purity 99.8%) and benzoyl peroxide (BP) were supplied by Sigma (Sigma-Aldrich Chemie, Steinheim, Germany). Phosphorus pentoxide (P_2O_5) and magnesium nitrate-6-hydrate ($Mg(NO_3)_2$), for sample conditioning, were obtained from Panreac Química, S.A. (Castellar del Vallès, Barcelona, Spain).

2.2. Chemical modification of PCL

The chemical modification of PCL by radical grafting reaction was carried out according to the methodology described by Laurienzo et al. [18] and Ortega-Toro et al. [17]. For this purpose, PCL was modified by incorporating benzoyl peroxide as the reaction catalyst, to make the α-carbon reactive. Two modification reactions have been

carried out: modification with maleic anhydride and glycidyl methacrylate to obtain PCL_{MG} (Fig. 1) and modification with only glycidyl methacrylate to obtain PCL_G (Fig. 1). Maleic anhydride can modulate the reaction avoiding polymerization of glycidyl methacrylate; giving rise to PCL bonded to both anhydride and glycidyl groups, with more polar molecular regions, as shown Figure 1. As reported in the previous study [17], the molar grafting ratio determined for maleic anhydride in PCL_{MG} from FTIR analysis was 4.5±0.9 % and the glycidyl methacrylate molar grafting in PCL_G was 4.3±0.4 %, determined from H^1 NMR analysis.

A Brabender plastograph (EC Plus, Duisburg, Germany) was used for the reaction, where 45 g of PCL, 2.5 g of M, 0.5 g of BP and 2.5 g of G were incorporated into the mixer at 100 ºC and maintained for 20 min at 32 rpm to functionalise the PCL with maleic anhydride and glycidyl methacrylate (PCL_{MG}). Modified PCL_{MG} was dissolved in 500 mL of chloroform and subsequently re-precipitated in excess of hexane, with the aim of removing any ungrafted reagents. The PCL functionalization with glycidyl methacrylate only (PCL_G) was performed with 45 g of PCL, 0.5 g of BP and 5 g of G. The reaction and purification were carried out following the same process previously described for PCL_{MG} synthesis. Both materials were kept in desiccator under vacuum for 12 h at 25 ºC, and frozen stored (-40 ºC) before using.

2.3. Experimental design and film preparation

Twelve film formulations were obtained: glycerol plasticized starch (S), pure PLA, and S-PLA blends with and without PCL_G or PCL_{MG} compatibilizers. Two levels of PLA in the blend films were considered (20 and 40% of starch substitution). In all films, glycerol was incorporated as 30 wt% of the starch and compatibilizers (PCL_G or PCL_{MG}) were added as 2.5 or 5 % of the total polymers (S plus PLA). The mass fraction

of each component in the dry blends and their sample identification codes are shown in Table 1.

The melt blending process was carried out in an internal mixer (HAAKE™ PolyLab™ QC, Thermo Fisher Scientific, Germany) at 160 °C, 50 rpm, for 10 min and 50 g of blend were processed in each batch. The obtained pastes were cut into pellets and conditioned at 25 ºC and 53% relative humidity (RH) for one week before the compression moulding to obtain the films. To this end, a hot plate press (Model LP20, Labtech Engineering, Thailand) was used. 4 g of the conditioned pellets were placed onto Teflon sheets and preheated for 3 min at 160 ºC and compression moulded for 1 min at 30 bars, followed by 3 min at 130 bars; thereafter, a 3 min cooling cycle was applied. Films were conditioned at 25 ºC and 53% RH for 1 week before their characterisation.

2.4. Film characterisation

2.4.1. Field emission scanning electron microscopy (FESEM)

A Field Emission Scanning Electron Microscope (FESEM Ultra 55, Zeiss, Oxford Instruments, U.K) was used to analyse the cross-section microstructure of the films. Samples were maintained in desiccators with P_2O_5 for 2 weeks at 25 °C, then, film samples were fractured and adequately placed on support stubs and coated with platinum. Observations were carried out at 1.5 kV.

2.4.2. X-Ray diffraction

The X-Ray diffraction patterns of the different samples were obtained by means of a diffractometer (XRD, Bruker AXS/D8 Advance) between 2θ: 5° and 30° with a step size of 0.05, using Kα Cu radiation (λ: 1.542 Å), 40 kV and 40 mA. The degree of

crystallinity (Xc) of the samples was estimated from the ratio of crystalline peak areas and the integrated area of XR diffractograms and expressed as a percentage, using OriginPro 8.5 software, assuming Gaussian profiles for crystalline and amorphous peaks, as was reported by Ortega-Toro et al. [20].

2.4.3. Attenuated Total Reflectance-Fourier Transform Infrared (ATR-FTIR) spectroscopy

The chemical groups in the films were identified through vibration type by the attenuated reflectance ATR-FTIR analysis (Nicolete 5700, Thermo Fisher Scientific Inc., MA, USA) in the range of 4000-400 cm^{-1} with a resolution of 4 cm^{-1}. Samples were recorded as an average of 64 scans.

2.4.4. Thermal behaviour

Differential Scanning Calorimetry (DSC 1 Star^e System, Mettler-Toledo Inc., Switzerland) was performed to analyse the phase transitions in the polymer matrices. Samples (7-9 mg) were placed into aluminium pans and sealed and the lid was perforated to ease the sample water release. They were submitted to a heating cycle from 25 ºC to 160 ºC; a cooling step from 160 ºC to 25 ºC, and a second heating cycle till 160 ºC, all of which at 10 ºC/min. In the first scan, the bonded water in the film was eliminated and, in the second heating cycle, the glass transition of starch and PLA was analysed.

The thermal stability of the samples was examined using a Thermogravimetric Analyzer TGA 1 Star^e System analyser (Mettler-Toledo, Inc., Switzerland). Samples (3-4 mg) were heated from 25 to 600 ºC at 20 ºC/min under nitrogen atmosphere (gas flow: 10 $mL.min^{-1}$). Initial degradation temperature (T_{Onset}) and peak temperature (T_{Peak}) were

200 studied using the STAR^e Evaluation Software (Mettler-Toledo, Inc., Switzerland), from
201 the first derivative of the resulting weight loss curves.
202
203 *2.4.5. Tensile properties*
204 A universal test machine (TA.XTplus model, Stable Micro Systems, Haslemere,
205 England) was used to study the tensile properties of the films following the ASTM
206 standard method D882 [21]. Conditioned samples (25 ºC, 53% RH) of 25 mm x 100
207 mm were mounted in the film-extension grips of the testing machine and stretched at 50
208 mm/min until break. Ten replicates were performed for each film formulation. Elastic
209 modulus (EM), tensile strength at break point (TS) and the elongation at break (ε) of the
210 films were determined from the stress-strain curves. The film thickness was taken into
211 account for the calculations.
212
213 *2.4.6. Oxygen permeability (OP), water vapour permeability (WVP) and moisture*
214 *content*
215 Oxygen barrier was determined in samples conditioned at 25 ºC and 53 % RH by using
216 OX-TRAN equipment, Model 2/21 ML (Mocon Lippke, Neuwied, Germany). A 50 cm^2
217 film area was used and the thickness was considered in all cases to obtain the OP
218 values. The oxygen transmission values were evaluated every 10 min until equilibrium.
219 The water vapour permeability (WVP) of the films was determined from a modification
220 of the gravimetric method E96-95 [21, 22]. For this purpose, Payne permeability cups
221 (Elcometer SPRL, Hermelle/s Argenteau, Belgium), 3.5 cm in diameter, were used. 5
222 mL of bidistilled water was added inside the cups and the film was fitted. Each cup was
223 placed into a desiccator with 53% RH by using a saturated solution of magnesium
224 nitrate. This was placed into a chamber with controlled temperature at 25 ºC. The cups

were weighed periodically (±0.0001g) and the water vapour transmission rate (WVTR) was determined from the regression analysis of weight loss data *vs.* time. From this data, WVP was obtained as described by Ortega-Toro et al. [20].

The equilibrium moisture content of the conditioned films was obtained by the sample drying in a natural convection oven (J.P. Selecta, S.A. Barcelona, Spain) for 24 h at 60 °C. Then, they were placed in a desiccator at 25 ºC with P_2O_5 (0% RH) for one week to lead the water content to a value of nearly 0. The moisture content of each sample was calculated from the total weight loss of conditioned samples, and expressed as a percentage of dry solids.

2.4.7. Optical properties

The internal transmittance (Ti) of the films, related with the sample transparency, was obtained by applying the multiple scattering Kubelka-Munk theory [24]. Ti (eq. 1) was determined from the reflection spectra (400-700 nm) with a spectorocolorimeter CM-3600d (Minolta Co., Tokyo, Japan) on black and white backgrounds. Internal transmittance at 460 nm was chosen to compare the values of the samples.

$$T_i = \sqrt{(a - R_0)^2 - b^2} \quad (1)$$

where R_0 is the reflectance of the film on the ideal black background. The parameters a and b were calculated by eqs. (2) and (3).

$$a = \frac{1}{2}\left(R + \frac{R_0 - R + R_g}{R_0 R_g}\right) \quad (2)$$

$$b = \sqrt{a^2 - 1} \quad (3)$$

where R is the reflectance of the sample layer backed by a known reflectance R_g.

The gloss of the samples was measured at an incidence angle of 85º, following the ASTM standard D523 method [25], using a flat surface gloss meter (Multi-Gloss 268, Minolta, Germany). All results are expressed as gloss units (GU), relative to a highly polished surface of black glass standard with a value near to 100 GU.

2.5. Statistical analysis

Statgraphics Centurion XVI software (Manugistics Corp., Rockville, Md.) was used to perform the statistical analyses of the results by means of analysis of variance (ANOVA). Fisher's least significant difference (LSD) procedure was used at the 95% confidence level.

3. Results and discussion

3.1. Nano- and micro-structural properties

No covalent bonds between grafted PCL and PLA or starch were expected considering the potential reactive groups of the different polymers and the melt blending conditions, without catalyst. However, given the amphiphilic nature of the grafted PCL (with polar and non-polar regions), molecular interactions between the hydrophobic regions of polyesters could be expected as well as the formation of hydrogen bonds between the starch hydroxyl groups and polar heads (epoxide or anhydride groups) of grafted PCL, according to the molecular structures shown in Fig. 1. In this sense, the interfacial location of the grafted PCL, could favour the dispersion of both polymers, decreasing the interfacial energy through the interactions with both PLA and starch. It is remarkable that PCL_{MG} molecular structure contains more polar groups and so, a higher

hydrophilic-lipophilic balance can be expected for this molecule. This implies that interactions with starch would be more favoured in this case.

FTIR analysis was carried out to assess potential differences in the chemical interactions between the film components, especially when compatibilizers were present. Fig. 2 shows the FTIR-ATR spectra of pure S and PLA and of the different blend films with and without different ratios of compatibilizers. The starch sample spectrum shows the characteristic broadband at around 3280 cm^{-1} which corresponds to stretching vibration types of -OH groups of amylose, amylopectin, glycerol and adsorbed water. Other bands relative to starch are identified at 2925 cm^{-1} and 1076-923 cm^{-1}, associated with C-H and C-O stretching, respectively; the peaks at 860, 760 and 570 cm^{-1} are assigned to the vibrational absorption peaks of the C-H bond [14, 27]. Another characteristic broad peak at 1645 cm^{-1} was observed, concerning the vibration mode of water molecules that are tightly absorbed in the amorphous regions of starch; this did not appear in the pure PLA sample in line with its more hydrophobic nature and appeared with lower relative intensity in the compatibilised blends [17]. In the PLA spectrum, the C=O stretching vibrations and the vibrations of C-O bonds of ester groups display peaks at 1745 and 1267 cm^{-1}, respectively. The peak at 863 cm^{-1} is attributed to the -C-C- stretching of the amorphous phase and peaks at 1452 and 1361 cm^{-1} are related to the deformation vibrations of the $-CH_2-$ and $-CH_3$ groups, respectively. The -C-O-C- stretching of the ester groups (1182 cm^{-1}), the C-O stretching (1128 and 1078 cm^{-1}) and the -OH bending (1039 cm^{-1}) are also observed [30, 14].

In S-PLA blend films, the combination of characteristic peaks of each polymer was observed in the same spectrum, with the corresponding changes in the relative intensity. A slight displacement of the carbonyl peak of PLA from 1745 (net PLA) to 1747 or 1749 cm^{-1} (S-PLA films), was observed in non-compatibilised blends. This

displacement was more marked in the compatibilised blends (1751-1755 cm^{-1}) and may be attributed to the different chain interactions promoted in the blends with or without compatibilizers and suggests that the presence of functionalized PCL could affected the packing of the PLA chains due to the hydrophobic interactions with the compatibilizers. No peaks associated with the functionalized PCL were observed in the compatibilised samples due to its lower proportion in the blends. The carbonyl PCL peak could overlap with the carbonyl band of PLA and no typical bands of the grafted compounds were observed. As reported in previous studies, the PCL_{MG} spectrum exhibited peaks at 1780 and 1850 cm^{-1} attributed to the stretching of the carbonyl group of the grafted anhydride, and the PCL_G spectrum shows a characteristic peak at 910 cm^{-1} related to the stretching vibration of epoxy ring C-O bonds [30, 17].

In order to analyse the effect of compatibilisation on polymer crystallization in the films, Fig. 3 shows the X-ray diffraction patterns as well as the percentage of crystallinity of the different films. PLA did not show crystalline peaks, coherent with their initial amorphous nature, whereas starch films exhibited three typical crystalline peaks at 2θ values of around 12.9º, 17.1º and 19.8º, attributed to the crystalline form of amylose type V as reported by other authors [8, 20, 29, 30]. The amylose V-type structure can be Vh (hydrated) with diffraction peaks at 12.6° and 19.4º, and Va (anhydrous) with peaks at 13.2° and 20.6°, which are formed by the crystallization of amylose in single helices involving glycerol or lipids [14, 17]. Blend films only exhibited the crystalline peaks of V-type amylose, thus revealing that only this polymer crystallized in the blends and no induced crystallization of PLA occurred. The characteristic crystalline peaks of PCL are around 2θ of 21.6º, 22.2º and 23.3º [17] and these peaks were not observed in any compatibilised sample. This can be due to the relatively low proportion of PCL in the blends, or to the inhibition of crystallization

brought about by the anchoring of the polar groups and their interfacial location. Then, the crystallization pattern of the starch in blend samples was not altered by the presence of amorphous PLA and/or compatibilizers. As regards the degree of crystallinity, the incorporation of PLA with and without compatibilisers slightly enhanced amylose crystallization, since taking the global reduction of the film's starch ratio into account, the degree of crystallinity with respect to that of net starch films increased by about 1% in the blends with 20 or 40% PLA, although in absence of compatibilizer, this change could be no significant. However, the incorporation of compatibilizers promoted the crystallinity of starch up to about 6 (with 40% PLA) or 7% (with 20% PLA), when referred per mass unit of starch. This could be attributed to a specific nucleating effect of the compatibilizer, enhancing the crystallization capacity of the amylose chains. This could be attributed to the hydrogen bond formation with the epoxide or anhydride groups of the grafted PLC, which could promote the amylose helical conformation and crystalline aggregation. The degree of crystallinity affects the film properties, such as stiffness, resistance, stretchability or brittleness and barrier properties, among other aspects.

Fig. 4 shows the FESEM micrographs of the cross-section of S-PLA blends with and without compatibilizers at both PLA proportions. In almost the all blend films, PLA domains appear dispersed in the continuous starch matrix, except films with 40% PLA and PCLG at 2.5 and 5%, in which PLA formed the continuous phase while starch domains were dispersed and densely packed in the PLA phase. The PLA phase (dispersed or continuous) exhibited less brittle fracture behaviour than that observed for the starch phase, showing some flakes typical of a more rubbery material. In the non-compatibilised samples, films with 40% PLA show the greatest number of PLA domains with a more flaky structure, interrupting the starch matrix.

In the morphological analysis of FESEM micrographs, different aspects were considered: the size of dispersed domains and the smoothness of the film fractured surface. The latter reveals the union force between the components through the presence of prevalent fracture zones. In terms of the effectiveness of the polymer compatibilization, a lower size of dispersed domains and a higher smoothness of the fracture surface could indicate higher efficiency of the compatibilizers. The former is related with the fact that compatibilizer reduce efficiently the interfacial energy favouring the mixing degree and the second indicates that compatibilizer allows for establishing adequate union forces at the interfacial area (interfacial adhesion) between both continuous and dispersed phase. Low interfacial adhesion would provoke weaken structures with poor mechanical performance.

As regards non-compatibilized blends, dispersed domains are bigger and separation at the interface during fracture occurred as can be observed in the micrographs. Both aspects agree with the lack of compatibility of the polymers, which generates big domains of dispersed PLA with weaken adhesion forces at the interface, thus promoting separation of the phases during the film fracture. The incorporation of both compatibilizers into the blends provoked a positive change in the film structure, with a notable reduction in the size of the PLA domains and no separation of the dispersed domains at the interface during the film fracture. These beneficial effects were more marked for 5 % of compatibilizer for both PCL_G and PCL_{MG}, in agreement with the action of a higher number of amphiphilic molecules. In blends with 20% PLA, films with 5% of PCL_G exhibited the most homogenous structure, with the best dispersion level of PLA in the starch matrix. With higher ratio of PLA in the blends (40 % substitution of starch), a phase inversion was promoted by the action of PCL_G. At both concentrations, the incorporation of PCL_G led to a PLA continuous phase where the

374 starch domains were embedded in the PLA matrix, this being clearer at the highest level
375 of compatibilizer. In this case, the starch domains appeared more finely distributed in
376 the PLA continuous phase, which indicates the most effective role of the compatibilizer
377 at this highest ratio. The occurrence of phase inversion for the highest ratio of PLA with
378 PCL_G could be attributed to the lower hydrophilic-lipophilic balance of the
379 compatibilizer molecule that would favour the continuity of the more hydrophobic
380 phase of PLA. In dispersed systems, it is well known that phase inversion is related with
381 the relative volume fraction of the immiscible liquid phases, the hydrophilic-lipophilic
382 balance (HBL) of the interfacial material and temperature. The most polar phase, at
383 volume fraction higher than 75% in the blend, is expected to be the continuous phase.
384 However, when the hydrophobic nature of the interfacial material increases, phase
385 inversion can occur at low volume fraction of the non-polar phase at a determined
386 temperature. From the molecular structure of compatibilizers (Fig. 1) a more
387 hydrophobic nature can be deduced for PLC_G. Therefore, the formation of a PLA (more
388 hydrophobic) continuous phase could be expected for the highest PLA volume fraction
389 in the blend, in contrast with that expected for the more polar compatibilizer such as
390 PCL_{MG}.
391 So, the kind of compatibilizer and its percentage in the blends, as well as the polymer
392 ratio, affected the microstructure of the blend films [26]. The interactions between the
393 hydroxyl groups of the starch chains and the hydroxyl, carboxyl or anhydride groups
394 grafted in the PCL chain contributed to polymer compatibilization, as also reported by
395 Ortega-Toro et al. [17] and Haque et al. [27] for other starch-polyester blends
396 compatibilized with PCL_G or PCL_{MG}. Orozco et al. [28] also observed a good
397 compatibilizing effect for PLA functionalized with maleic anhydride on blend films of
398 potato starch and PLA. All the compatibilized blends reflected better adhesion

properties between PLA and starch, based on the interactions between the polar groups grafted in the PLA chain and starch.

3.2. Thermal analysis

The thermogravimetric analysis (TGA) provides information on the thermal stability of polymers, so the maximum temperature that supports the material can be known [9]. Table 2 summarises the initial degradation temperature (Onset) and the temperature at the maximum degradation rate (Peak) of the different film formulations, and TGA and DTG curves are shown in Fig. 5. The initial degradation temperature of the pure starch film is around 264 ºC; at this point the weight loss is accentuated, as can be seen in Fig. 5, until reaching the maximum degradation rate at 299 ºC. During the degradation process, the dehydration of the hydroxyl groups in the glucose ring takes place; moreover, ether bonds and unsaturated structures are formed by the thermal condensation of the hydroxyl groups of the starch chains, eliminating water and low molecular weight substances [31]. The PLA sample had an initial degradation temperature above that of pure starch, and a maximum degradation rate at 317ºC similar to that previously reported by Sanyang et al. [32]. The S-PLA blends at both ratios, with and without compatibilizers, show three degradation phases of differing intensities, depending on the composition of the mixtures without the complete miscibility of components. The first phase, between 125-205 ºC, corresponds to the degradation of low molecular weight components, such as plasticizers (glycerol); the main second phase, between 225-325 ºC, is attributable to the overlapped degradation of starch and PLA, since both polymers possess similar degradation temperatures, and the third phase, above 330 °C (in samples with compatibilizers), would mainly correspond to the degradation of the grafted PCL with higher degradation temperatures (341-381 ºC,

[17]), partially overlapped with the final degradation of PLA. The degradation temperature of the pure PCL is between 300-400 °C and the graft of glycidyl methacrylate and maleic anhydride can partially inhibit the crystallization of the PLC, which promotes degradation at slightly lower temperatures [17].

Table 2 shows that both the initial degradation temperature and the temperature at the maximum degradation rate of the polymers were closer to the corresponding temperatures of the starch, due to its higher ratio in the blends. However, the main peak was wider and extended at higher temperatures, especially when blends contained 40% PLA, reflecting the greater contribution of the PLA degradation to the main peak. For these samples, in fact, the shoulder at about 340 ºC, corresponding to the degradation of the grafted PCL, overlapped the PLA final degradation to a greater extent, but at similar temperatures. This behaviour indicates that the thermal degradation of the different polymers is scarcely influenced by the blending effect. The lack of a significant effect of grafted PCL on thermal stability of both starch and PLA indicates that polymers degrade as pure polymers. So, no crosslinking by covalent bonds occurred in the blends due to the action of compatibilizers, as deduced from FTIR spectra, and they only favoured the polymer mixing by decreasing the interfacial energy, forming finer dispersions with smaller size of the dispersed domains, thus increasing the interfacial area.

Table 2 also shows the glass transition temperatures (T_g) of the starch and the PLA for the different formulations, obtained from the second heating scan to avoid effects of thermal history of the composites. The T_g of the starch is around 100ºC, as reported by other authors [20, 33], and there were no significant differences between the S and S-PLA formulations. However, compatibilizers exert an anti-plasticization effect in the starch phase by increasing its T_g, which was slightly more pronounced for PCL_G.

Usually, the addition of plasticizers causes a decrease in the glass transition temperature by increasing the free volume in the matrix, which allows the molecular mobility of the polymers [34]. The increase in the Tg of the starch in the compatibilised blends at both percentage of PLA can be attributed to the chemical interactions between the hydroxyl groups of starch and the grafted polar groups of PCL, which restrict molecular mobility in this phase, affecting the glass transition temperature [17]. In contrast, the addition of compatibilizers had a slight plasticizing effect on the PLA phase, provoking a decrease in its glass transition temperature. Hydrophobic interactions between the non-polar regions of grafted PCL and PLA, could weaken interaction forces of the PLA chains and, additionally, the non-grafted PCL regions could plasticize the polyester phase by a partial miscibility effect. This behaviour also demonstrates the interactions of compatibilizers with both polymers, enhancing their dispersion.

3.3. Mechanical properties

The tensile properties (elastic modulus: EM, tensile strength at break: TS and the elongation at break: ε) of the formulations are shown in Table 3. Starch had the lowest value of EM, which indicates that these films are the least stiff and resistant. However, the starch tends to retrograde during storage, the films becoming stiffer and less flexible due to the formation of crystalline zones [35]. As regards PLA, despite its high tensile strength and elastic modulus, which are comparable with those of conventional polymers such as PET or PS, it is a very brittle material with less than 10% elongation capacity [12]. In blend films without a compatibilizer, an increase in EM and a decrease in ε compared to the pure starch films was observed, which implies an increase in the strength and stiffness of the material, with a reduction in its extensibility. However, the greatest % of PLA implied less resistant, less extensible films with similar stiffness to

474 the films with the lowest PLA ratio. This could be explained in terms of the film
475 microstructure, where the PLA phase was dispersed in a continuous starch matrix. The
476 cohesion force of the continuous matrix greatly contributed to the film's strength and an
477 increase in the volume of the dispersed phase reduced the overall film cohesiveness,
478 despite the higher strength of the dispersed PLA. In compatibilised blends with 20%
479 PLA, a significant increase in EM (~2 times, when using $PCL_{2.5MG}$) and TS (~1.5 times,
480 when using $PCL_{2.5G}$) with respect to the non-compatibilised blends was observed.
481 However, a decrease in the film elongation at break was noted in compatibilised films
482 when PCL_G at 2.5% and PCL_{MG} at 5% were used. Compatibilized samples with 40%
483 PLA exhibited lower values of EM, TS and ε compared to those containing 20% PLA,
484 as commented on for the non-compatibilized blends, which can be attributed to the
485 increase in the volume of the dispersed phase. This factor is particularly relevant for
486 films compatibilized with PCL_G, as commented on above, which provoked the phase
487 inversion in the polymer blend, the PLA becoming the continuous matrix, but with a
488 high volume fraction of dispersed starch that weakened the strength of the PLA
489 continuous phase. As a result of the structural effects, no remarkable differences could
490 be established for the mechanical parameters of films with 40% PLA, regardless of the
491 presence or type of compatibilizers. Therefore, from a mechanical point of view, the
492 greater substitution of starch by PLA did not represent any advantage.
493 The rule of mixtures estimates mechanical properties (e.g. tensile strength or elastic
494 modulus) of polymer blends as the linear combination of the respective properties of the
495 components multiplied by the volume fraction in the blend. The properties of the
496 homogenous blends tend to follow this correlation, but mechanical behaviour of
497 materials based in immiscible polymers deviate from this rule due to their complex
498 morphology and the resulting micromechanical deformation process [19]. Then, as

499 expected, the studied blends did not follow the rule of mixtures, although their
500 mechanical behaviour was highly improved with the presence of compatibilizers with
501 respect to the non-compatibilized blends.
502 In blends with 20% PLA, the values of elongation at break were higher than those found
503 by Zuo et al. [36], by compatibilizing S-PLA blends by means of starch esterification
504 with maleic anhydride; however they obtained TS values of around 38 MPa. The
505 improved mechanical behaviour of blend films with grafted-PCL compatibilizers
506 reflects the better dispersion and interfacial adhesion of the polylactic acid in the starch
507 matrix, depending on the concentration and type of compatibilizer, as shown in the
508 FESEM micrographs. Ortega-Toro et al. [17] also used grafted PCL with G and MG to
509 compatibilize S-PCL blends in an 80:20 ratio and obtained improved mechanical
510 properties as the concentration of compatibilizer in the mixture increased.
511
512
513 *3.4. Moisture content and barrier properties*
514 The moisture content, water vapour permeability (WVP) and oxygen permeability of the
515 films are shown in Table 4. The moisture content of the films was consistent with the
516 different hydrophilic character of the polymers, although starch substitution by PLA did
517 not lead to the expected reduction in the water sorption capacity of the films, whose
518 equilibrium water content values were similar to those of the net starch film.
519 Pure starch films showed the highest values of WVP in the range previously reported by
520 other authors [20, 37]. The partial substitution of starch by PLA in the blends, with and
521 without compatibilizers, implied a WVP reduction of about 33 or 50% for 20 and 40%
522 PLA, respectively. The decrease in the WVP in films with starch continuous phase can
523 be associated with the increase in the tortuosity factor for mass transfer caused by the

524 dispersion of the hydrophobic PLA domains [17]; the higher the volume fraction of
525 dispersed phase, the greater the tortuosity factor and the permeability reduction.
526 However, in films with 40% PLA and 5% $PCL_{G,}$ the reduction was more marked (67%).
527 This can be attributed to the continuity of the hydrophobic PLA phase, as can be
528 observed in Fig. 4, which limited the transport of water molecules due to the lower
529 water solubility in this continuous phase.
530 As concerns the oxygen permeability, blend films were more permeable than net starch
531 films, but much lesser permeable than net PLA films. No significant differences in OP
532 were observed for 20 and 40% PLA in the non-compatibilized blends, whose higher
533 values with respect to the starch can be explained by the presence of a less polar phase
534 in the matrix which promote the oxygen solubility. The incorporation of compatibilizers
535 significantly decreases the OP for both PLA ratios with respect to non-compatibilized
536 samples. The reduction was about 40% in every case regardless of the ratio of PLA and
537 the kind and amount of compatibilizer. This decrease could be attributed to the better
538 dispersion of polymers which enhanced the tortuosity factor of the matrix, thus limiting
539 the diffusion of the gas molecules through the matrix. Likewise, as reported by Ortega-
540 Toro et al. [17], the interfacial location of the grafted PCL and interactions with PLA
541 can hinder the diffusion of the gas molecules into the PLA domains, thus affecting the
542 overall permeability of the films.
543
544 *3.5. Optical properties*
545 Fig. 6 shows the internal transmittance (Ti) of the films in the wavelength range of 400-
546 700 nm as an indicator of the film transparency to VIS radiation. The mean values and
547 standard deviation of Ti at 460 nm (Ti) and gloss at 85º are shown in Fig. 7. The S-PLA
548 blend films with and without compatibilizer exhibited lower values of Ti than pure PLA

549 or starch films, coherently with the formation of a heterogeneous system with a polymer
550 dispersed phase in a continuous phase of the other polymer; both phases have a different
551 refractive index, which implies light scattering effects with the consequent increase in
552 the film opacity. This can be considered positive for food applications as it is potentially
553 able to protect the food, reducing the light induced oxidation reactions. In most cases,
554 the addition of compatibilizers had no significant effect on the Ti values, except for
555 three blends which exhibited the lowest Ti values and the highest gloss. These samples
556 were the blend with 20% PLA and 5% PCL_G and the two blends with 40% PLA and
557 PCL_G at 2.5 and 5%. These differences must be associated with the particular film
558 microstructure. In the first case, the better PLA dispersion in the starch matrix, with the
559 reduced size of PLA domains, as shown in FESEM micrographs, will cause a greater
560 light scattering effect; this will give rise to less transparency in the films, at the same
561 time as the better PLA dispersion will promote lower surface irregularities and higher
562 gloss in the films. The two samples with 40% PLA with lower transparency
563 corresponded to the inverted structures, where PLA constituted the continuous phase
564 with a high amount of dispersed starch phase, which will provoke a more marked light
565 scattering effect, reducing the film transparency. In these cases, the continuity of the
566 PLA phase enhanced the film gloss. Similar effects have been found by other authors
567 for blends of PLA and plasticized starch [15].
568

569 **4. Conclusions**

570 The starch-PLA matrices compatibilized with grafted PCL presented a better dispersion
571 of the PLA in the continuous starch phase, especially for the highest amount of
572 compatibilizer. The use of PCL_G provoked a phase inversion in the matrix when 40% of
573 starch was substituted by PLA. Interactions between polymers and compatibilizers

574 could be deduced from microstructural, thermal and spectral data. The compatibilized
575 blend films exhibited higher values of elastic modulus than pure starch films, but they
576 were less extensible, with similar tensile strength at break, the values depending on the
577 PLA ratio and the type and concentration of compatibilizer. From the mechanical point
578 of view, the film formulation containing 20% PLA and 5% PCL_G exhibited good tensile
579 strength and great extensibility, being suitable for packaging purposes. The WVP was
580 reduced by blending up to 33 or 50% for 20 and 40% PLA, respectively, although films
581 with 40% PLA and 5% PCL_G, exhibited a marked reduction (67%). The incorporation
582 of compatibilizers significantly decreased the OP by about 40% respect to non-
583 compatibilized samples, regardless of the % of PLA and the kind and amount of
584 compatibilizer. Therefore, substituting 20% of the starch by PLA and incorporating 5%
585 PCL_G would be a good strategy to obtain films that are useful for food packaging; the
586 starch phase provided the films with an excellent oxygen barrier capacity, while PLA
587 enhanced the mechanical resistance and reduced the water vapour permeability. In
588 particular, dry or partially dehydrated products and fatty or oxidation-sensitive foods
589 could be adequately packaged with these films, thus improving their preservation.
590
591 **Acknowledgements**
592 The authors thank the Ministerio de Economía y Competitividad (Spain) for the
593 financial support provided through Project AGL2016-76699-R. The authors also wish to
594 thank the Electron Microscopy Service of the UPV for their technical assistance.
595
596 **Data availability**
597 The raw/processed data required to reproduce these findings cannot be shared at this
598 time due to legal or ethical reasons.

References

[1] C. Brigham, Biopolymers: Biodegradable alternatives to traditional plastics, in: B. Török, T. Dransfield (Eds.), Green chemistry, Elsevier Inc., Amsterdam, 2018, pp. 753-770.

[2] C. Ingrao, V. Siracusa, Quality- and sustainability-related issues associated with biopolymers for food packaging applications: a comprehensive review, in: N. Gopal Shimpi (Ed), Biodegradable and Biocompatible Polymer Composites, Woodhead Publishing, 2018, pp. 401-418.

[3] A.B. Balaji, H. Pakalapati, M. Khalid, R. Walvekar, R, H. Siddiqui, Natural and synthetic biocompatible and biodegradable polymers, in: N. Gopal Shimpi (Ed.), Biodegradable and biocompatible polymer composites, Woodhead Publishing, United Kingdom, 2017, pp. 3–32.

[4] M.J. Fabra, A. López-Rubio, J.M. Lagarón, Biopolymers for food packaging applications, in: M. R. Aguilar De Armas, J. S. Román (Eds.), Smart polymers and their applications, Woodhead Publishing, United Kingdom,2014, pp. 476-509.

[5] M. Bassas-Galia, S. Follonier, M. Pusnik, M. Zinn, Natural polymers: a source of inspiration, in: G. Perale, J. Hilborn (Eds.), Bioresorbable polymers for biomedical applications, Woodhead Publishing**.** United Kingdom, 2017, pp. 31-64.

[6] L. Jiang, J. Zhang, Biodegradable and biobased polymers, in: M. Kutz (Ed.), *Applied Plastics Engineering Handbook,* William Andrew, New York, 2017, pp. 127-143.

[7] K. Koch, K. Starch-based film. In M. Sjöö, L. Nilsson (Eds), Starch in food, Woodhead Publishing, 2018, pp. 747-767.

[8] R. Ortega-Toro, J. Contreras, T. Talens, A. Chiralt, Physical and structural properties and thermal behaviour of starch-poly(e-caprolactone) blend films for food packaging, Food Packag. and Shelf Life 5 (2015) 10-20.

624 [9] S. Collazo-Bigliardi, R. Ortega-Toro, A. Chiralt, Isolation and characterisation of
625 microcrystalline cellulose and cellulose nanocrystals from coffee husk and
626 comparative study with rice husk, Carbohydr. Polym. 191 (2018) 205-215.
627 [10] S. Collazo-Bigliardi, R. Ortega-Toro, A. Chiralt, Properties of Micro- and nano-
628 reinforced biopolymers for food applications, in: T. Gutiérrez (Ed.), Polymers for
629 food applications, Springer, 2018, pp. 61-99.
630 [11] R. Ortega-Toro, J. Bonilla, P. Talens, A. Chiralt, Starch-based materials in food
631 packaging, in: M. A. Villar, S.E. Barbosa, M.A. García, L.A. Castillo, O.V. López
632 (Eds.), Future of starch-based materials in food packaging, Aspen Publishers, 2017,
633 pp. 257-312.
634 [12] J. Muller, C. González-Martínez, A. Chiralt, A. Combination of poly(lactic) acid
635 and starch for biodegradable food packaging, *Mater.* 10 (2017) 952-974.
636 [13] M. Murariu, P. Dubois, PLA composites: From production to properties, Adv.
637 Drug Deliv. Rev. 107 (2016) 17-46.
638 [14] J. Muller, C. González-Martínez, A. Chiralt, Poly(lactic) acid (PLA) and starch
639 bilayer films, containing cinnamaldehyde, obtained by compression moulding. Eur.
640 Polym. J. 95 (2017) 56-70.
641 [15] P. Müller, J. Bere, R. Fekete, J. Móczó, B. Nagy, M. Kállay, B. Gyarmati, B.
642 Pukánszky, Interactions, structure and properties in PLA/plasticized starch blends.
643 Polym. 103 (2016) 9-18.
644 [16] N. Le Bolay, A. Lamure, N. Gallego, A. Subhani, How to combine a hydrophobic
645 matrix and a hydrophilic filler without adding a compatibilizer-Co grinding
646 enhances use properties of renewable PLA-starch composites, Chem. Eng. and
647 Process. 56 (2012) 1-9.

[17] R. Ortega-Toro, G. Santagata, G. Gomez d'Ayala, P. Cerruti, P. Talens, A. Chiralt, M. Malinconico, Enhancement of interfacial adhesion between starch and grafted poly(ε-caprolactone), Carbohydr. Polym. 147 (2016) 16-27.

[18] P. Laurienzo, M. Malinconico, G. Mattia, G. Romano, Synthesis and characterization of functionalized crosslinkable poly(ε-caprolactone), Macromol. Chem. and Phys. 207 (2006) 1861-1869.

[19] B. Imre, L. García, D. Puglia, F. Vilaplana, Reactive compatibilization of plant polysaccharides and biobased polymers: Review on current strategies, expectations and reality, Carbohydr. Polym. 209 (2019) 20-37.

[20] R. Ortega-Toro, S. Collazo-Bigliardi, P. Talens, A. Chiralt, Influence of citric acid on the properties and stability of starch-polycaprolactone based films, J. Appl. Polym. Sci. 42220 (2016) 1-16.

[21] ASTM, Standard test method for tensile properties of thin plastic sheeting. Standard Designations: D882, Annual book of ASTM standards. Philadelphia, PA: American Society for Testing and Materials (2001).

[22] ASTM, Standard test methods for water vapor transmission of materials. Standard Designations: E96-95, In Annual books of ASTM, Philadelphia, PA: American Society for Testing and Materials, 1995, pp. 406-413.

[23] T.H. McHugh, R. Avena-Bustillos, J.M. Krochta, J. M, Hydrophobic edible films: Modified procedure for water vapour permeability and explanation of thickness effects. J.l of Food Sci. 58(4) (1993) 899-903.

[24] J.B. Hutchings, Food color and appearance (2nd ed.), Gaithersburg, Maryland, Aspen Publishers Inc., USA, 1999.

671 [25] ASTM, Standard test method for specular gloss. In Designation (D523).annual
672 book of ASTM standards, vol. 06.01. PA: American Society for Testing and
673 Materials Philadelphia, 1999.
674 [26] M. Akrami, I. Ghasemi, H. Azizi, M. Karrabi, M. Seyedabadi, A new approach in
675 compatibilization of the poly(lactic acid)/thermoplastic starch (PLA/TPS) blends.
676 Carbohydr. Polym. 144 (2016) 254-262.
677 [27] M. Haque, M.E. Errico, G. Gentile, M. Avella, M. Pracella, Functionalization and
678 compatibilization of poly(ε-caprolactone) composites with cellulose microfibres:
679 morphology, thermal and mechanical properties, Macromolecular Mater. and Engi.
680 297(10) (2012) 985-993.
681 [28] V.H. Orozco, W. Brostow, W. Chonkaew, B.L. Lopez, Preparation and
682 characterization of poly (Lactic acid)-g-maleic anhydride + starch blends,
683 Macromol. Symp. 277 (2009) 69-80.
684 [29] L. Castillo, O. López, C. López, N. Zaritzky, M.A. García, S. Barbosa, M. Villar,
685 Thermoplastic starch films reinforced with talc nanoparticles, Carbohydr. Polym.
686 95(2) (2013) 664-674.
687 [30] S.M. Davachi, B.S. Heidari, I. Hejazi, J. Seyfi, E. Oliaei, A. Farzaneh, H. Rashedi,
688 Interface modified polylactic acid/starch/poly ε-caprolactone antibacterial
689 nanocomposite blends for medical applications, Carbohydr. Polym. 155 (2017)
690 336-344.
691 [31] O.V. López, L.A. Castillo, S.E. Barbosa, M.A. Villar, M. A. García, Processing–
692 properties–applications relationship of nanocomposites based on thermoplastic corn
693 starch and talc, Polym. Compos. 39(4) (2018) 1331-1338.

694 [32] M.L. Sanyang, S.M. Sapuan, M. Jawaid, M.R. Ishak, J. Sahari, Development and
695 characterization of sugar palm starch and poly (lactic acid) bilayer films.
696 Carbohydr. Polym., 146 (2016) 36-45.
697 [33] A. Tampau, C. González-Martínez, A. Chiralt, Release kinetics and antimicrobial
698 properties of carvacrol encapsulated in electrospun poly-(ε-caprolactone)
699 nanofibres. Application in starch multilayer films, Food Hydrocoll. 79 (2018) 158-
700 169.
701 [34] P.Y. Mikus, S. Alix, J. Soulestin, M.F. Lacrampe, P. Krawczak, X. Coqueret, P.
702 Dole, Deformation mechanisms of plasticized starch materials, Carbohydrate
703 Polym. 114 (2014) 450-457.
704 [35] R. Ortega-Toro, A. Jiménez, P. Talens, A. Chiralt, Properties of starch-
705 hydroxypropyl methylcellulose based films obtained by compression molding.
706 Carbohydr. Polym. 109 (2014) 155-165.
707 [36] Y. Zuo, J. Gu, L. Yang, Z. Qiao, H. Tan, Y. Zhang, Preparation and
708 characterization of dry method esterified starch/polylactic acid composite materials,
709 Intern. J. of Biol. Macromol. 64 (2014) 174-180.
710 [37] S. Collazo-Bigliardi, R. Ortega-Toro, A. Chiralt, Reinforcement of thermoplastic
711 starch films with cellulose fibres obtained from rice and coffee husks, J. Renew.
712 Mater. 6(6) (2018) 599-610.

Figure captions

Fig. 1. Molecular structure of grafted PCL (PCL_G and PCL_{MG}). Adapted from Ortega-Toro et al. [17].

Fig. 2. FTIR-ATR spectra of S-PLA films with 20 or 40 wt% PLA, compatibilized or not with 5% of PCL_G or PCL_{MG}.

Fig. 3. X-ray diffraction patterns and degree of crystallinity (Xc, %) of S-PLA films with 20 or 40 wt% PLA, compatibilized or not with 2.5 and 5% of PCL_G or PCL_{MG}.

Fig. 4. FESEM micrographs of the cross-section of S-PLA films with 20 or 40 wt% PLA, compatibilized or not with 2.5 and 5% of PCL_G or PCL_{MG}. Starch (S) and PLA (P) phases are indicated in the micrographs.

Fig. 5. TGA (a) and DTGA (b) curves of S-PLA films with 20 or 40 wt% PLA, compatibilized or not with 2.5 and 5% of PCL_G or PCL_{MG}.

Fig. 6. Internal transmittance (Ti) spectra of TPS-PLA films with 20 or 40 wt% PLA, compatibilized or not with 2.5 and 5% of PCL_G or PCL_{MG}.

Fig. 7. Mean values and standard deviation of internal transmittance at 460 nm (Ti) and gloss (85º) values of S-PLA films with 20 or 40 wt% PLA, compatibilized or not with 2.5 and 5% of PCL_G or PCL_{MG}.

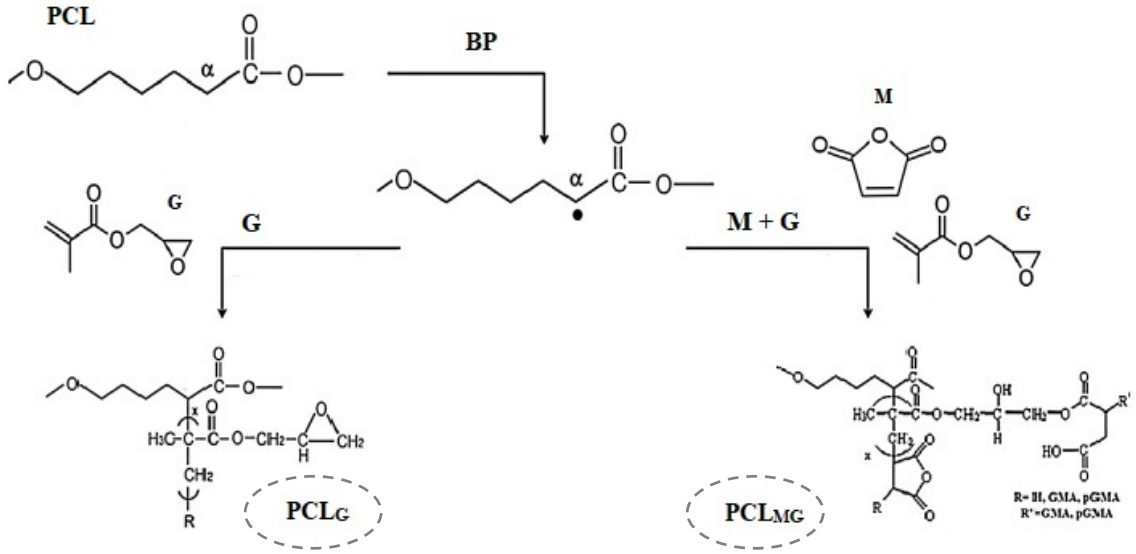

Fig. 1.

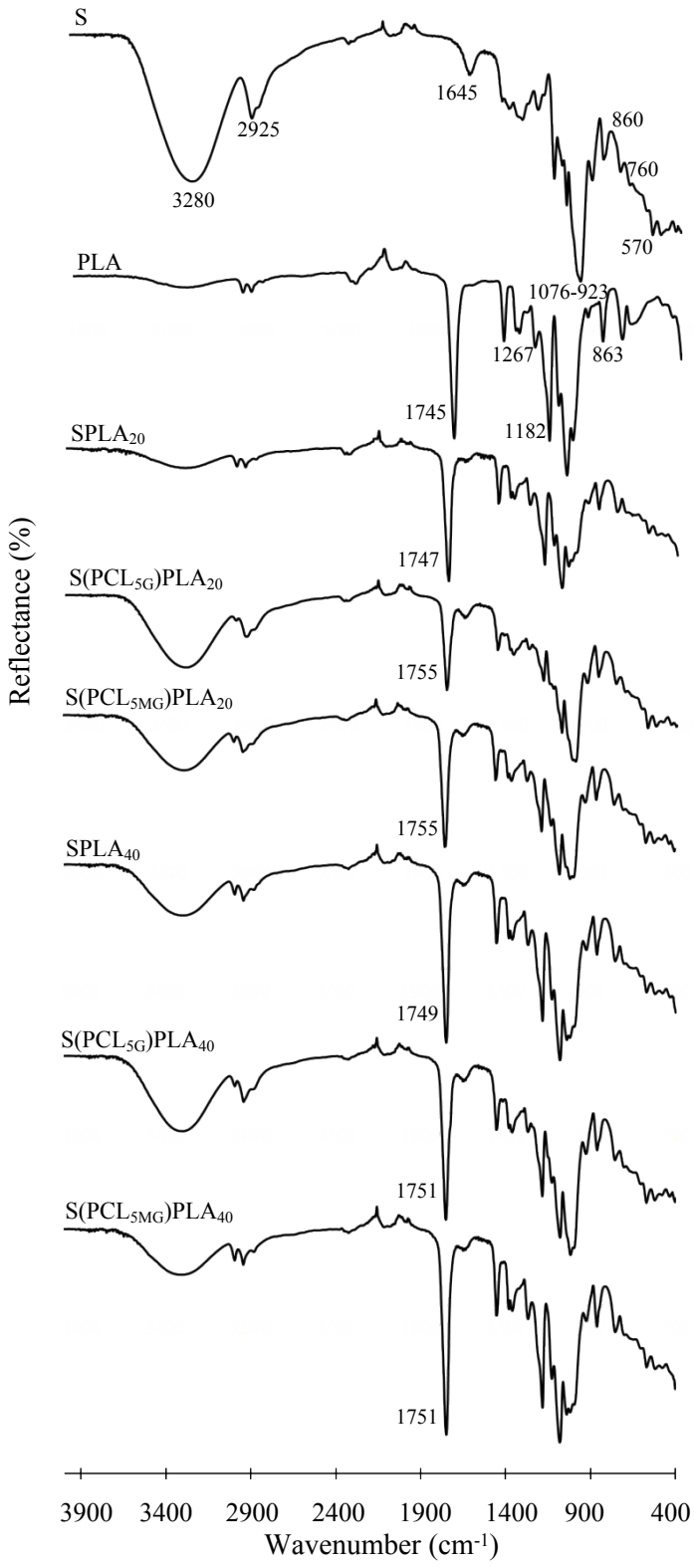
S
3280
2925
1645
860
760
570
PLA
1076-923
1267
863
1745
1182
SPLA20
1747
S(PCL5G)PLA20
1755
S(PCL5MG)PLA20
1755
SPLA40
1749
S(PCL5G)PLA40
1751
S(PCL5MG)PLA40
1751
Reflectance (%)
3900 3400 2900 2400 1900 1400 900 400
Wavenumber (cm-1)

Fig. 2.

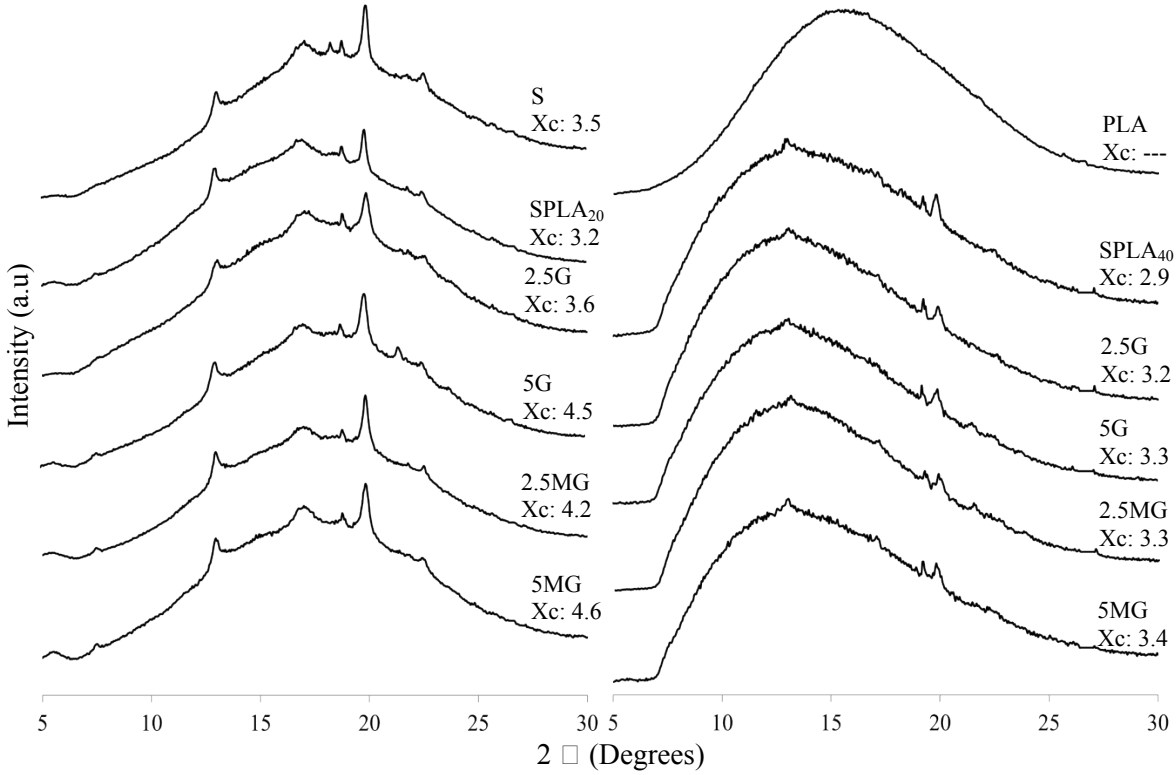
S
Xc: 3.5
SPLA20
Xc: 3.2
2.5G
Xc: 3.6
5G
Xc: 4.5
2.5MG
Xc: 4.2
5MG
Xc: 4.6
PLA
Xc: ---
SPLA40
Xc: 2.9
2.5G
Xc: 3.2
5G
Xc: 3.3
2.5MG
Xc: 3.3
5MG
Xc: 3.4
Intensity (a.u)
5
10
15
20
25
30
2 □ (Degrees)

Fig. 3.

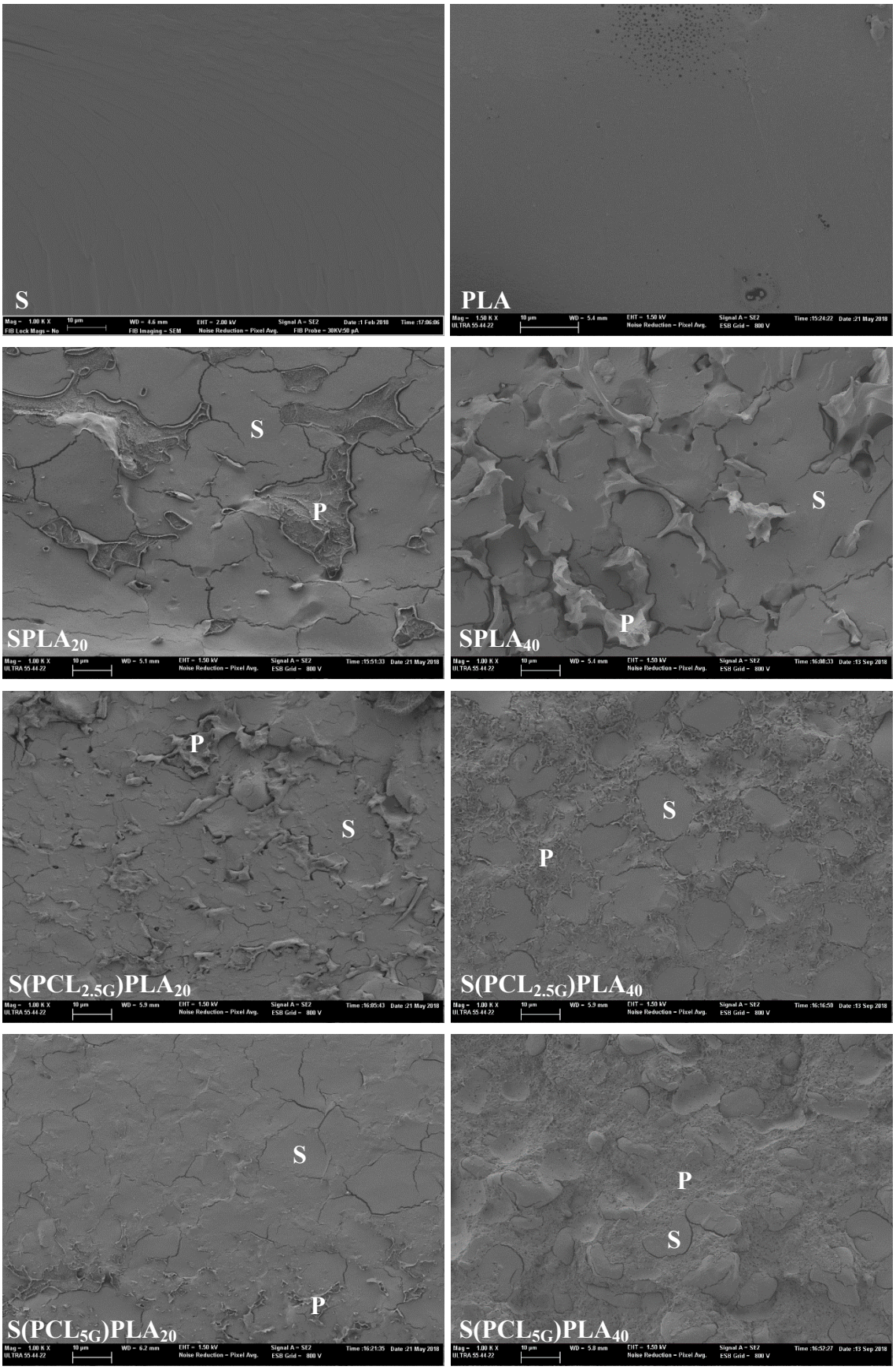
S
PLA
S
P
SPLA20
S
P
SPLA40
P
S
S(PCL2.5G)PLA20
S
P
S(PCL2.5G)PLA40
S
P
S(PCL5G)PLA20
P
S
S(PCL5G)PLA40

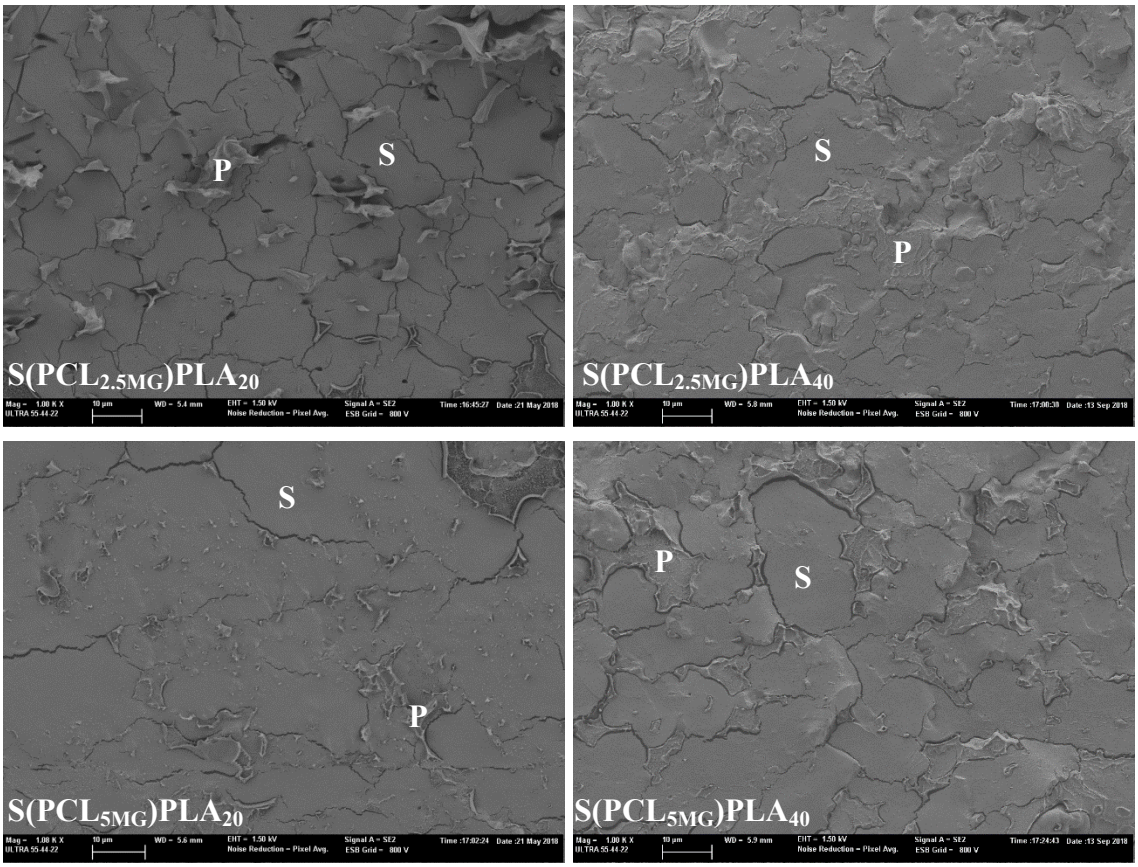
P
S
S(PCL2.5MG)PLA20
S
P
S(PCL2.5MG)PLA40
S
P
S(PCL5MG)PLA20
P
S
S(PCL5MG)PLA40

Fig. 4.

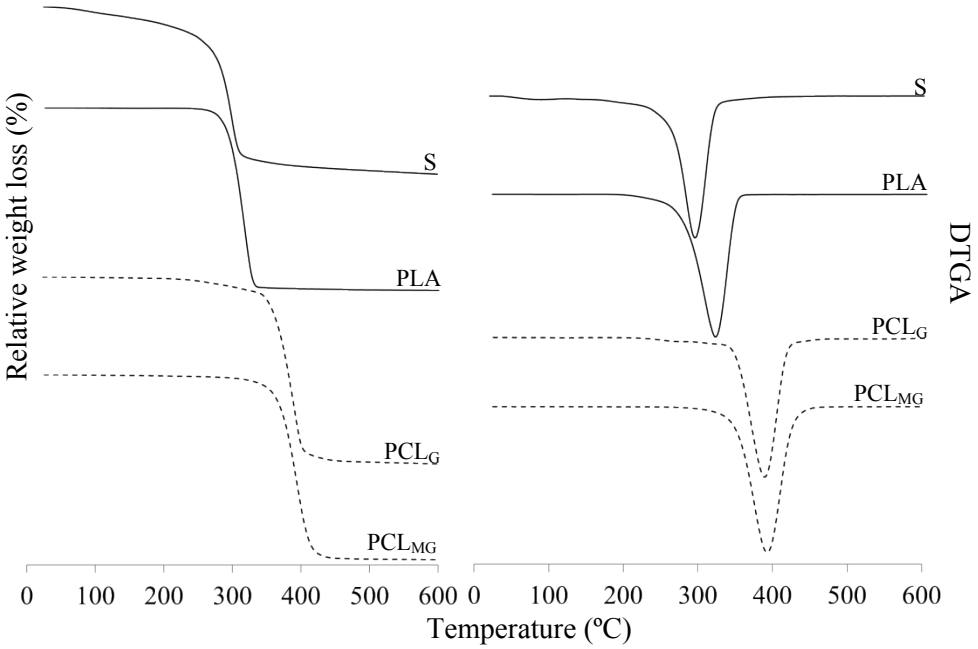
Relative weight loss (%)
S
PLA
PCL$_G$
PCL$_{MG}$
DTGA
0 100 200 300 400 500 600
Temperature (ºC)

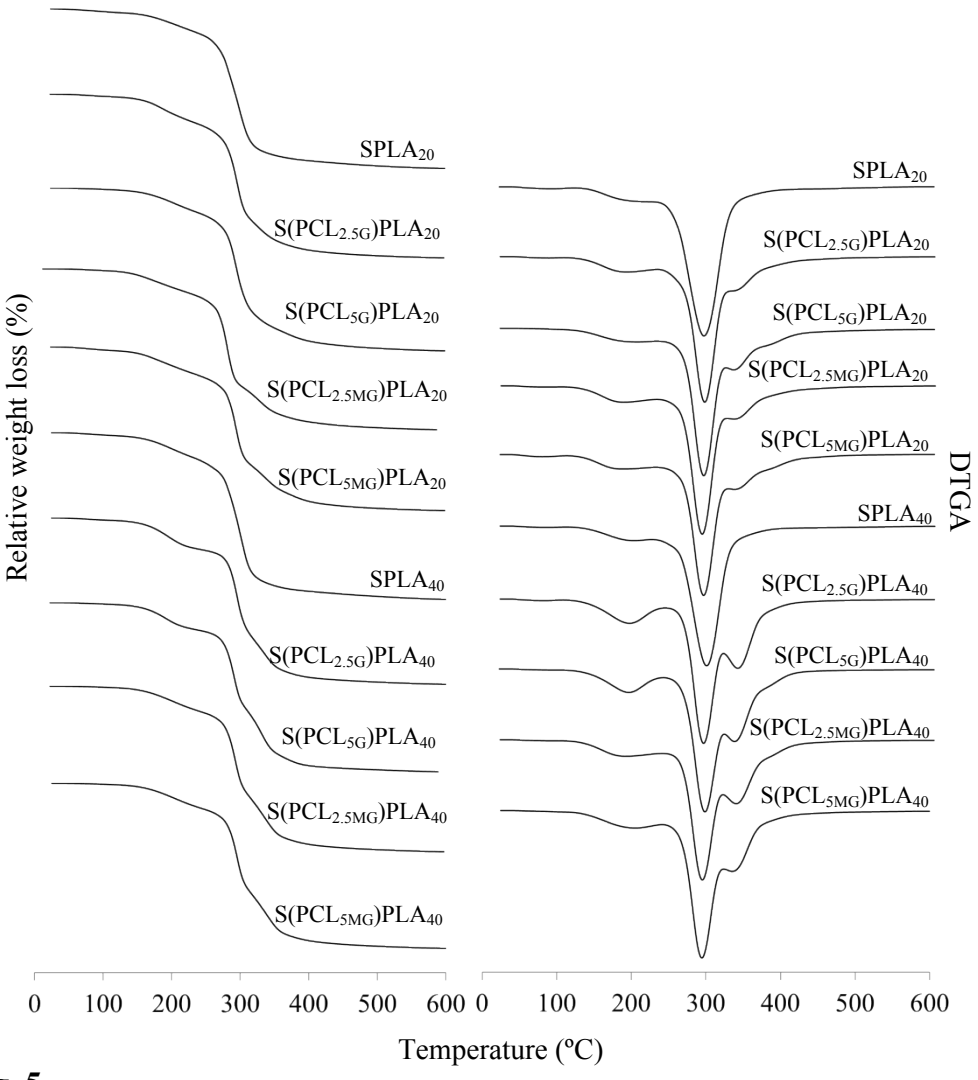
Relative weight loss (%)
SPLA$_{20}$
S(PCL$_{2.5G}$)PLA$_{20}$
S(PCL$_{5G}$)PLA$_{20}$
S(PCL$_{2.5MG}$)PLA$_{20}$
S(PCL$_{5MG}$)PLA$_{20}$
SPLA$_{40}$
S(PCL$_{2.5G}$)PLA$_{40}$
S(PCL$_{5G}$)PLA$_{40}$
S(PCL$_{2.5MG}$)PLA$_{40}$
S(PCL$_{5MG}$)PLA$_{40}$
DTGA
0 100 200 300 400 500 600
Temperature (ºC)

Fig. 5.

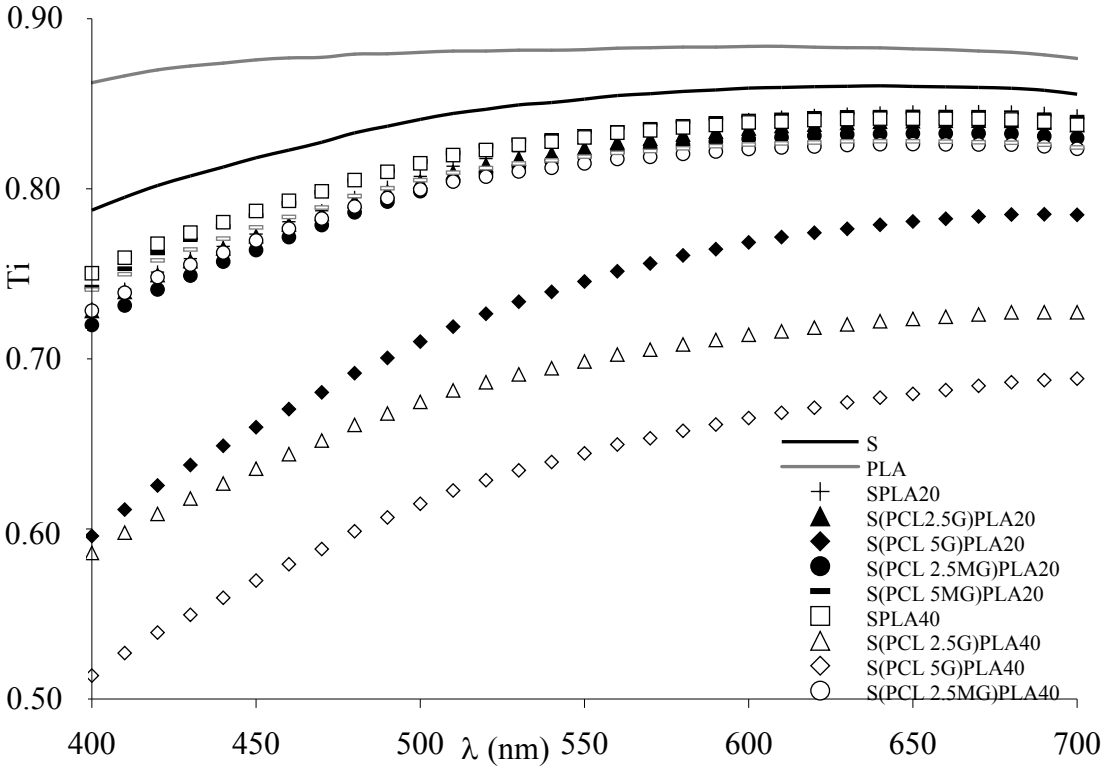
0.90
0.80
0.70
0.60
0.50
Ti
400
450
500
λ (nm)
550
600
650
700
S
PLA
SPLA20
S(PCL2.5G)PLA20
S(PCL 5G)PLA20
S(PCL 2.5MG)PLA20
S(PCL 5MG)PLA20
SPLA40
S(PCL 2.5G)PLA40
S(PCL 5G)PLA40
S(PCL 2.5MG)PLA40

Fig. 6.

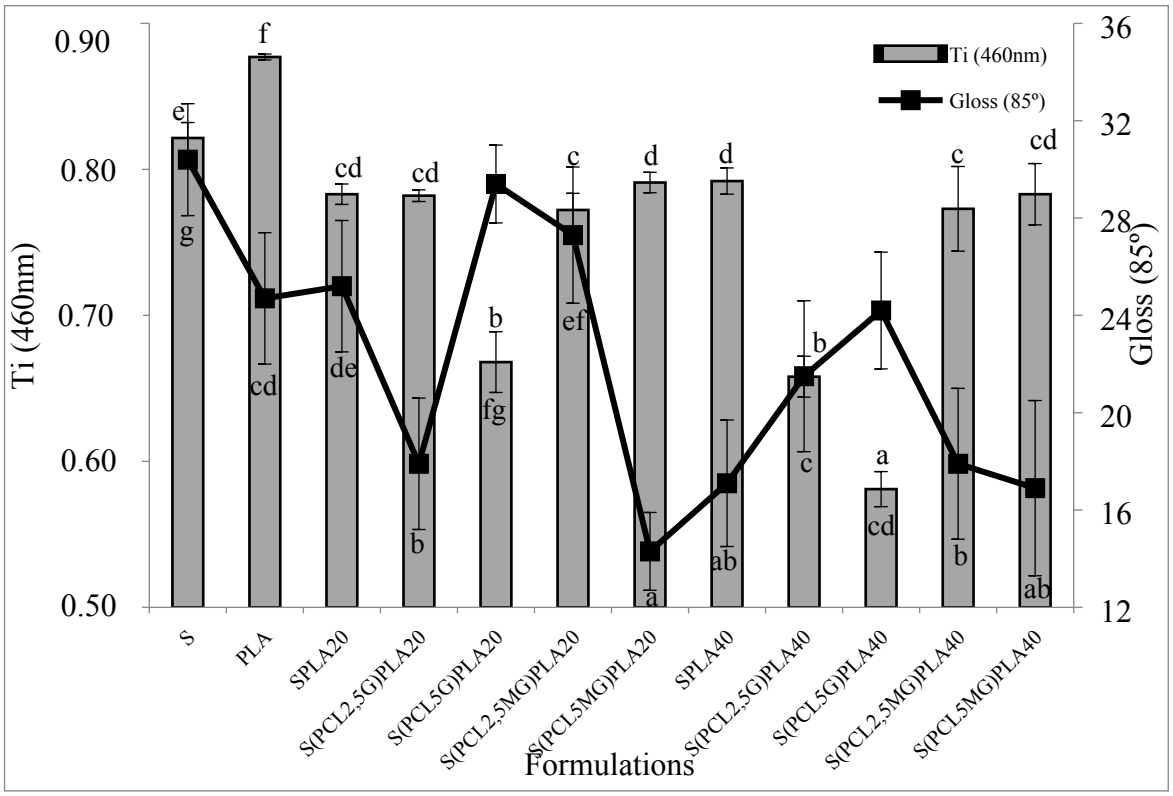
Ti (460nm)
Gloss (85º)
Ti (460nm)
Gloss (85º)
0.90
0.80
0.70
0.60
0.50
36
32
28
24
20
16
12
e
f
cd
cd
c
d
d
c
cd
g
cd
de
b
fg
ef
a
ab
b
c
cd
b
ab
b
a
S
PLA
SPLA20
S(PCL2,5G)PLA20
S(PCL5G)PLA20
S(PCL2,5MG)PLA20
S(PCL5MG)PLA20
SPLA40
S(PCL2,5G)PLA40
S(PCL5G)PLA40
S(PCL2,5MG)PLA40
S(PCL5MG)PLA40
Formulations

Fig. 7.

Table 1. Mass fraction (Xi, g compound/g dried Film) of the different components: Starch (S), glycerol (Gly), grafted poly(ε-caprolactone) with glicidyl methacrylate (PCL_G), grafted poly(ε-caprolactone) with maleic anhydride and glycidyl methacrylate (PCL_{MG}) and polylactic acid (PLA) at 20 or 40 wt.% of starch.

Formulations	X_S	X_{Gly}	X_{PCL-G}	X_{PCL-MG}	X_{PLA}
S	0.7692	0.2308	-	-	-
PLA	-	-	-	-	1.0000
S PLA_{20}	0.6667	0.200	-	-	0.1333
S($PCL_{2.5G}$)PLA_{20}	0.6536	0.1961	0.0196	-	0.1307
S(PCL_{5G})PLA_{20}	0.6410	0.1923	0.0385	-	0.1282
S($PCL_{2.5MG}$)PLA_{20}	0.6536	0.1961	-	0.0196	0.1307
S(PCL_{5MG})PLA_{20}	0.6410	0.1923	-	0.0385	0.1282
S PLA_{40}	0.5882	0.1765	-	-	0.2353
S($PCL_{2.5G}$)PLA_{40}	0.5764	0.1729	0.0202	-	0.2305
S(PCL_{5G})PLA_{40}	0.5650	0.1695	0.0395	-	0.2260
S($PCL_{2.5MG}$)PLA_{40}	0.5764	0.1729	-	0.0202	0.2305
S(PCL_{5MG})PLA_{40}	0.5650	0.1695	-	0.0395	0.2260

Table 2. Mean values and standard deviation of onset and peak temperatures of thermal degradation and glass transition temperature (Tg; midpoint in the second heating scan on DSC) of S-PLA dry films compatibilised or not with 2.5 and 5% of PCL_G or PCL_{MG}.

Samples	[125-205]ºC		[255-360]ºC		[339-387]ºC	Second heating scan	
	Onset (ºC)	Peak (ºC)	Onset (ºC)	Peak (ºC)	Peak (ºC)	$T_{g\ Starch}$ (ºC)	$T_{g\ PLA}$ (ºC)
S	-	-	264 ± 2^{b}	299 ± 4^{c}	-	98.6 ± 0.1^{a}	-
PLA	-	-	278 ± 0.5^{f}	317 ± 5^{b}	-	-	55.3 ± 0.2^{e}
S PLA_{20}	165 ± 3^{g}	201 ± 4^{g}	256 ± 1^{a}	296 ± 0.5^{a}	-	99.3 ± 0.1^{a}	52.8 ± 0.7^{d}
S($PCL_{2.5G}$)PLA_{20}	149 ± 0.2^{f}	185 ± 3^{cd}	271 ± 0.3^{de}	296 ± 1^{a}	341 ± 2^{a}	105.0 ± 3.0^{c}	50.1 ± 0.1^{bc}
S(PCL_{5G})PLA_{20}	146 ± 4^{ef}	195 ± 2^{f}	269 ± 1^{cde}	296 ± 1^{a}	381 ± 6^{b}	105.6 ± 0.8^{c}	49.3 ± 0.7^{ab}
S($PCL_{2.5MG}$)PLA_{20}	129 ± 2^{ab}	180 ± 0.2^{ab}	269 ± 2^{bcde}	292 ± 2^{a}	343 ± 2^{a}	101.1 ± 0.2^{ab}	49.6 ± 0.2^{abc}
S(PCL_{5MG})PLA_{20}	128 ± 3^{a}	176 ± 0.2^{a}	270 ± 0.3^{de}	294 ± 1^{a}	343 ± 0.2^{a}	103.0 ± 4.0^{bc}	50.1 ± 0.1^{bc}
S PLA_{40}	139 ± 0.4^{cd}	189 ± 3^{de}	265 ± 3^{bc}	297 ± 1^{a}	-	98.2 ± 0.3^{a}	52.1 ± 0.9^{d}
S($PCL_{2.5G}$)PLA_{40}	144 ± 1^{def}	195 ± 1^{f}	272 ± 0.2^{e}	294 ± 1^{a}	342 ± 2^{a}	105.0 ± 1.0^{c}	49.9 ± 0.7^{bc}
S(PCL_{5G})PLA_{40}	149 ± 3^{f}	196 ± 2^{fg}	270 ± 4^{de}	293 ± 3^{a}	342 ± 2^{a}	104.4 ± 0.5^{bc}	49.5 ± 0.3^{abc}
S($PCL_{2.5MG}$)PLA_{40}	135 ± 7^{bc}	183 ± 0.2^{bc}	266 ± 5^{bcd}	293 ± 1^{a}	345 ± 4^{a}	103.6 ± 0.4^{bc}	49.4 ± 0.4^{a}
S(PCL_{5MG})PLA_{40}	141 ± 2^{cde}	193 ± 1^{ef}	271 ± 0.2^{de}	294 ± 0.3^{a}	342 ± 2^{a}	103 ± 1^{bc}	50.5 ± 0.3^{c}

Different superscript letters within the same column indicate significant differences between formulations ($p < 0.05$).

Table 3. Mean values and standard deviation of tensile properties (EM: elastic modulus, TS: tensile strength at break and ε: extensibility) of conditioned (53% RH and 25 ºC) S-PLA films compatibilized or not with 2.5 and 5% of PCL_G or PCL_{MG}.

Formulation	EM (MPa)	TS (MPa)	ε (%)	Thickness (mm)
S	77 ± 15^{a}	5.2 ± 1.6^{bc}	64.9 ± 0.5^{h}	0.20 ± 0.02^{bc}
PLA	1370 ± 34^{g}	53.0 ± 2.0^{f}	4.3 ± 0.2^{a}	0.22 ± 0.01^{d}
S PLA_{20}	143 ± 20^{cd}	5.7 ± 0.7^{c}	17.5 ± 3.5^{f}	0.17 ± 0.02^{a}
S($PCL_{2.5G}$)PLA_{20}	312 ± 28^{f}	8.6 ± 0.3^{e}	9.6 ± 1.8^{d}	0.19 ± 0.01^{ab}
S(PCL_{5G})PLA_{20}	195 ± 35^{e}	7.6 ± 0.3^{d}	21.1 ± 1.9^{g}	0.19 ± 0.01^{bc}
S($PCL_{2.5MG}$)PLA_{20}	162 ± 39^{d}	5.9 ± 0.4^{c}	22.3 ± 2.1^{g}	0.17 ± 0.02^{a}
S(PCL_{5MG})PLA_{20}	318 ± 43^{f}	8.1 ± 0.7^{de}	7.2 ± 1.3^{bc}	0.18 ± 0.02^{a}
S PLA_{40}	112 ± 14^{bc}	4.3 ± 0.3^{ab}	6.5 ± 1.3^{b}	0.20 ± 0.01^{bc}
S($PCL_{2.5G}$)PLA_{40}	135 ± 13^{cd}	5.9 ± 0.7^{c}	8.0 ± 1.6^{bcd}	0.23 ± 0.02^{de}
S(PCL_{5G})PLA_{40}	101 ± 15^{ab}	8.1 ± 0.8^{de}	12.9 ± 1.5^{e}	0.24 ± 0.02^{e}
S($PCL_{2.5MG}$)PLA_{40}	98 ± 18^{ab}	4.3 ± 0.9^{ab}	8.9 ± 0.9^{cd}	0.20 ± 0.02^{cd}
S(PCL_{5MG})PLA_{40}	117 ± 14^{bc}	4.1 ± 0.6^{a}	5.8 ± 0.5^{ab}	0.21 ± 0.02^{bc}

Different superscript letters within the same column indicate significant differences among formulations ($p < 0.05$).

Table 4. Mean values and standard deviation of moisture content, water vapour permeability (WVP) and oxygen permeability (OP) of S-PLA conditioned (53% RH and 25 ºC) films compatibilised or not with 2.5 and 5% of PCL_G or PCL_{MG},.

Formulation	Moisture content (g water/g dried film)	WVP ($g \cdot mm \cdot kPa^{-1} \cdot h^{-1} \cdot m^{-2}$)	OP x10^{14} ($cm^3 \cdot m^{-1} \cdot s^{-1} \cdot Pa^{-1}$)
S	0.096 ± 0.007^{bc}	14.9 ± 0.4^{f}	10.3 ± 0.1^{a}
PLA	0.0025 ± 0.0004^{a}	0.158 ± 0.01^{a}	466.0 ± 3.0^{e}
S PLA_{20}	0.071 ± 0.003^{b}	10.2 ± 0.3^{de}	39.0 ± 1.0^{d}
S($PCL_{2.5G}$)PLA_{20}	0.068 ± 0.005^{b}	10.7 ± 0.7^{e}	24.0 ± 4.0^{bc}
S(PCL_{5G})PLA_{20}	0.065 ± 0.004^{b}	10.1 ± 0.4^{de}	19.9 ± 0.6^{b}
S($PCL_{2.5MG}$)PLA_{20}	0.074 ± 0.002^{b}	9.76 ± 1.0^{de}	20.9 ± 0.8^{bc}
S(PCL_{5MG})PLA_{20}	0.0649 ± 0.0014^{b}	9.4 ± 0.3^{d}	19.9 ± 0.3^{b}
S PLA_{40}	0.097 ± 0.010^{bc}	7.6 ± 0.3^{c}	43.4 ± 1.5^{d}
S($PCL_{2.5G}$)PLA_{40}	0.086 ± 0.004^{b}	7.5 ± 0.2^{c}	24.7 ± 3.3^{c}
S(PCL_{5G})PLA_{40}	0.088 ± 0.005^{b}	5.1 ± 0.2^{b}	22.1 ± 1.9^{bc}
S($PCL_{2.5MG}$)PLA_{40}	0.125 ± 0.003^{de}	7.1 ± 0.4^{c}	23.5 ± 0.5^{bc}
S(PCL_{5MG})PLA_{40}	0.137 ± 0.006^{e}	7.1 ± 0.8^{c}	22.6 ± 0.3^{bc}

Different superscript letters within the same column indicate significant differences among formulations ($p < 0.05$).

Highlights

- Grafted poly(ε-caprolactone) were an excellent compatibilizer to S-PLA blends
- Compatibilized blends presented a better dispersion of the PLA in the S phase
- The mechanical properties were enhanced with the addition of compatibilizers
- Compatibilizers decreased the oxygen permeability of the films
- 20% of PLA and 5% of PCL_G into S blend would be a good strategy to obtain films useful for food packaging